



Evaluation of *Alpinia galanga* and its active principle, 1'-aceto-chavicol acetate as eco-friendly corrosion inhibitors on mild steel in acidic medium

S. O. Ajeigbe^{1,3}, N. Basar¹, H. Maarof¹, A. M. Al-Fakih¹, M. A. Hassan¹, M. Aziz^{1,2,*}

1. Department of Chemistry, Faculty of Science, Universiti Teknologi Malaysia, 81310 Skudai, Johor, Malaysia

2. Advanced Membrane Technology Centre, Universiti Teknologi Malaysia, 81310 UTM Johor Bahru, Johor, Malaysia

3. SLT Department, Federal Polytechnic, PMB 55 Bida, Nigeria

Received 19 Sep 2016,
Revised 28 Feb 2017,
Accepted 02 Mar 2017

Keywords

- ✓ Corrosion inhibitors;
- ✓ electrochemical methods;
- ✓ quantum chemical;
- ✓ *Alpinia galanga*;
- ✓ adsorption

M. Aziz
madzlan@utm.my
+60197582000

Abstract

Plant extracts as corrosion inhibitors have been expansively explored and are found as an alternative to synthetic organic compounds. Crude hexane extract of *Alpinia galanga* rhizome and its major active constituent namely, 1'-aceto-chavicol acetate were investigated for their corrosion inhibition properties on mild steel in hydrochloric acid solution using weight loss, electrochemical and quantum chemical methods. Potentiodynamic polarization investigations revealed that the inhibitors performed as mixed inhibitors. The highest inhibition efficiency of 90.2% was achieved for crude hexane extract while 84.6% was obtained for 1'-aceto-chavicol acetate. The quantum chemical parameters calculated for 1'-aceto-chavicol acetate as the major compound of the plant gave good correlation with the experimental results. The effectiveness of the inhibitors was also supported using field emission scanning electron microscopy (FESEM). The mechanism of interaction of both the inhibitors on mild steel surface was found to conform to the Langmuir adsorption isotherm.

1. Introduction

Corrosion and its devastating effects in the industry is a major concern. Efforts geared toward ameliorating the menace of corrosion is an additional major concern for industrialists and researchers [1]. Several efforts have been made to control the menace of corrosion in which the use of corrosion inhibitors plays a prominent role [2]. Corrosion inhibitors are substances added in a minute quantity to an electrochemical system to reduce the rate of deterioration of the metal. Foremost amongst the inhibitors are organic compounds.

Previous studies have shown that most organic inhibitors act by adsorption at the metal/solution interface [3]. This phenomenon could take place either as electrostatic attraction between the charged metal and the charged inhibitor molecules; dipole-type interaction between uncharged electron pairs in the inhibitor with the metal; the π -electrons bonds interaction with the metal and combination of all of the above [4-6].

Heterocyclic organic compounds containing atoms of oxygen, nitrogen, sulphur, and phosphorus as heteroatoms have been used as corrosion inhibitors [7-9]. These inhibitors are highly efficient due to their excellent adsorption unto the metal surface. In addition, several factors like the functional groups, steric factors, molecular structures, aromaticity and electron density at donor atoms as well as temperature and pH of the corrosion medium influence the adsorption of these inhibitors on the metal surface.

There are various types of organic inhibitors that have been reported [3, 10-14]. In the various works adsorption has been shown to depend on certain physicochemical properties of the inhibitor group, such as functional groups, electron density at the donor atom, π -orbital character, and the electronic structure of the molecule. The work of [15] shows that the adsorption process is influenced by the electronic characteristics of the inhibitor, the

nature of the metal surface, steric effect, temperature and pressure of reaction, multilayer adsorption as well as varying degree of surface site activity.

Of recent, the use of synthetic organic inhibitors has been limited as a result of their high costs and environmental threats posed by their use. This has therefore motivated an alternative in the natural organic compounds [10].

Plants have been found to be repository of several thousands of organic compounds some of which bear resemblance with the commonly used organic corrosion inhibitors [3, 15-17]. Extracts and constituents of plants have been used by several corrosion practitioners to alleviate the menace of corrosion. Naturally occurring substances are cheap and renewable, biodegradable and do not contain heavy metals or other toxic chemicals and are therefore eco-friendly and hence ecologically acceptable [18].

Extracts of tobacco plant [19] have been reported to show remarkable corrosion inhibition of aluminium and steel in both salt and acidic solutions. Extracts from *Lansea coromandelica* leaves [20]; *Nauclea latifolia* [21]; *Piper longa* [22] *Coriandrum sativum* L [23]; *Medicago sativa* [24]; *Tinospora crispa* [25]; *Sida acuta* [26]; Ginko leaves [12]; Thyme leaves [27]; Apricot juice [28]; *Jasminum nudiflorum* Lindl [29]; Coffee senna [30] and several other plants have also been studied and found to be effective as corrosion inhibitors.

The active components of various plant extracts have also been studied for corrosion inhibition in which the phytochemical constituents of plants have shown varying level of corrosion inhibition. Arbutin, an active principle from *Artemisia pallens* [31], alkaloid extracts of *Oxandra asbeckii* [32], Henna plant [33] and its constituents, lawsone, gallic acid α -D-glucose and tannic acid were shown to inhibit corrosion of mild steel in hydrochloric acid solution. *Punica granatum* peel and its main constituents, ellagic acid and tannic acid [34] were also found to be effective corrosion inhibitors on mild steel in acidic solutions; *Aniba rosaeodora* plant [35, 36] with anibine as the major alkaloid has also been studied.

The rhizomes of *A. galanga*, a plant belonging to the Zingiberaceae family, commonly called greater galangal is selected in this study. The plant is known to possess antioxidant properties [36, 37] and have been used as an herb for medical purposes [38]. The major active compound in *A. galanga* is 1'-acetoxychavicol acetate (ACA) with structure in figure 1.

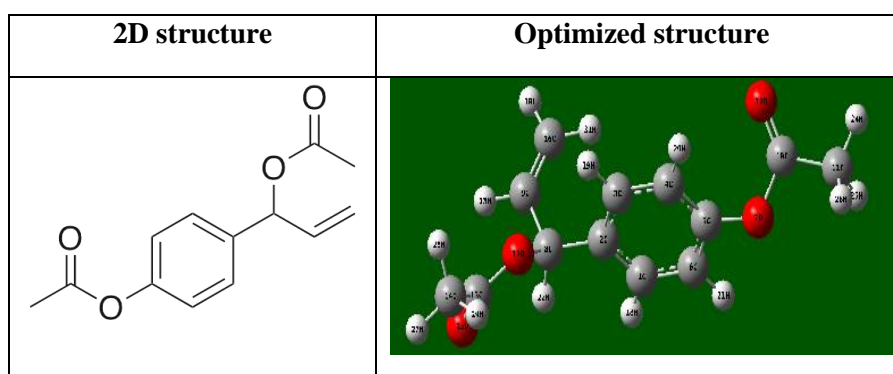


Figure 1: Structure of 1'-acetoxychavicol acetate (ACA)

Extracts of turmeric and ginger both belonging to the same family of Zingiberaceae as *A. galanga* have previously been investigated as green corrosion inhibitors [39, 40]. In their works, these plants have been found to have good corrosion inhibition efficiencies. *A. galanga* and its constituents, despite having good antioxidant properties and hence phytochemicals with good potentials for corrosion inhibition is yet to be exploited as a green corrosion inhibitor for mild steel in hydrochloric acid solution.

2. Experimental details

2.1. Materials

The rhizome of *A. galanga* was collected from Tanjong Karang, Selangor, Malaysia in 2015 and was identified at the Botany Department, UPM, Malaysia

2.2 Extraction and isolation of inhibitor

The rhizome of *A. galanga* (1.2 kg) was chopped, dried and ground into powder. The sample was extracted by soxhlet extraction with *n*-hexane as solvents for 18 hours. The extract was concentrated by rotary evaporator to yield *n*-hexane crude extract (CHE) (5.63 g, 0.47 %). The *n*-hexane crude extract (5.63 g) was fractionated by

Vacuum Layer Chromatography (VLC) using sintered funnel (10.5 cm diameter) and silica gel 230-400 mesh (170 g) and eluted by petroleum ether (PE), diethyl ether (Et₂O) and methanol with increasing polarity to afford 25 fractions. The Thin Layer Chromatography (TLC) was performed to all fractions and similar refractive index (R_f) were combined to give 8 fractions (ALG1-ALG8). The fraction ALG4 (2.02 g) was further purified by Column Chromatography (CC) using silica gel 70-230 mesh (60 g) and packed into column (3.0 cm diameter) with eluent system PE:Et₂O to yield 1'-acetoxychavicol acetate (ACA) (0.51 g, 9.06%) as colourless liquid..

2.3 Metal specimen preparation

Pre-cut mild steel specimens of dimension (2.0cm x 2.0cm x 0.25cm) with the composition (wt. %: 0.036 C; 0.172 Mn; 0.0146 P; 0.108 Ni; 0.0538 Cr; 0.082 Cu and Fe balance) were used for the experiments. Prior to every measurement, the samples were abraded with a series of silicon carbide abrasive paper (grades 180, 400, 800, 1200 and 1500). The specimens were then degreased with acetone, rinsed in distilled water, dried and stored in the desiccator in readiness for weight loss and electrochemical measurements.

2.4. Corrosion medium

The corrosion solution of 1 M HCl used was prepared by dilution of analytical reagent grade 37% HCl with distilled water. The CHE and ACA used were dissolved and sonicated in the 1 M HCl at different concentration ranging from 100 to 1000 ppm for the crude extract and the isolated compound (ACA). The 1 M HCl also served as the blank solution in the experiments.

2.5. Weight loss Method

After weighing accurately, the specimens were immersed in 100 ml of 1 M HCl with and without the addition of different concentrations of inhibitors for 3 hours. The mild steel specimens were then taken out, washed with distilled water and acetone, dried and weighed accurately. The average weight loss of three measurements was obtained. The determination was carried out at room temperature (27 ± 2 °C). The corrosion rate and the inhibition efficiency ($IE_{WL}\%$) of CHE and ACA on the mild steel sample were calculated respectively using Equations 1 and 2 as follows:

$$R_c = \frac{\Delta W}{S \cdot t} \quad (1)$$

Where R_c , ΔW , S and t are the corrosion rate, change in weight of mild steel specimen before and after immersion, surface area and time of immersion respectively.

$$IE_{WL} (\%) = 1 - \frac{W_{inh}}{W_{blank}} \times 100 \quad (2)$$

W_{inh} and W_{blank} are values of the weight loss with and without the addition of the inhibitors respectively.

2.6. Electrochemical experiments

Electrochemical studies were performed in a classical three-electrode cell of 250 ml capacity at room temperature (27 ± 2 °C). Mild steel coupons with an exposed area of 1 cm² served as the working electrode, with a platinum counter electrode and saturated calomel electrode (SCE) as the reference electrode. All electrochemical measurements were recorded at open circuit potential (OCP) after the immersion of mild steel specimen for 30 minutes in the test solution [41].

2.6.1. Potentiodynamic polarization studies

Potentiodynamic polarization measurements were performed using the AUTOLAB model PGSTAT 30 instrument. The polarization curves were carried out from cathodic and anodic potentials of ± 0.25 V with respect to the open circuit potential at a sweep rate of 1 mVs⁻¹. The linear Tafel segments of the anodic and cathodic curves were extrapolated to corrosion potential (E_{corr}) to obtain the corrosion current densities (I_{corr}). In each measurement, a fresh working electrode was used. Triplicate runs were performed for each experiment to obtain reproducible data.

Before polarization measurements, the working electrodes were immersed into the test solution and left for 30 minutes at the open-circuit potential (OCP). Polarization data were analysed using GPES electrochemical software and corrosion current density values were obtained by Tafel extrapolation method. The inhibition efficiencies at different inhibitor concentrations were calculated using Equation 3.

$$IE_{PDP}(\%) = \frac{I_{corr} - I_{corr(inh)}}{I_{corr}} \times 100 \quad (3)$$

I_{corr} and $I_{corr(inh)}$ are the corrosion current densities in the absence and presence of inhibitor, respectively [42].

2.6.2. Electrochemical Impedance Spectroscopy

Impedance studies were carried out using VersaSTAT 3 instrument. The measurements of AC impedance were carried out at the corrosion potential (E_{corr}) with frequency ranging from 100,000 to 0.01 Hz at an amplitude of 10 mV and scan rate of 10 points per decade. The inhibition efficiency was calculated from the values of charge transfer resistance (R_{ct}) by using Equation 4:

$$IE_{EIS}(\%) = \frac{R_{ct(inh)} - R_{ct}}{R_{ct(inh)}} \times 100 \quad (4)$$

Where R_{ct} and $R_{ct(inh)}$ are the charge transfer resistance in the absence and presence of inhibitor, respectively.

2.7. Field emission scanning electron microscopy

The surface morphological changes of mild steel in the inhibited and uninhibited acid solutions were assessed by using Field emission scanning electron microscopy (FESEM). Finely polished mild steel specimens were immersed in 1 M HCl solution in the absence of inhibitor and also separately in 250 ppm for both CHE and ACA. The specimens were retrieved after a period of 3 hours and cleaned with distilled water and acetone and then dried for surface examination.

3. Results and Discussion

3.1. Characterization of 1'-Acetoxychavicol acetate

The colourless liquid gave the following peaks; $R_f = 0.50$ (PE: $Et_2O = 4: 1$); 1H NMR ($CDCl_3$, 400 MHz): δ 7.39 (2H, d, $J = 8.8$ Hz, H-3, H-5), 7.10 (2H, d, $J = 8.8$ Hz, H-2, H-6), 6.28 (1H, d, $J = 5.6$ Hz, H-1'), 6.00 (1H, ddd, $J = 16.4$ Hz, 10.0 Hz, 5.6 Hz, H-2'), 5.32 (1H, dt, $J = 16.4$ Hz, 1.2 Hz, H-3'a), 5.27 (1H, dt, $J = 10.0$ Hz, 1.2 Hz, H-3'b), 2.12 (3H, s, CH_3), 2.31 (3H, s, CH_3); EIMS m/z (rel. int.): 234 [M^+ , $C_{13}H_{14}O_4$] (5), 192 (81), 150 (94), 132 (100), 77 (12).

3.2. Weight loss method

Results of weight loss measurements were taken at the normal room temperature of 27 °C in the presence of different concentrations of the inhibitors. The inhibition efficiencies were calculated and shown in Table 1.

Table 1: Corrosion rate and % Inhibition efficiency of CHE and ACA on mild steel at various concentrations in 1 M HCl by weight loss measurement

Inhibitor	Inh. Conc. (ppm)	Wt. Loss (mg)	Corr. Rate ($mgcm^{-2}h^{-1}$)	Inh. Eff. (%)
Blank	0	60.8	2.0267	-
CHE	100	20.7	0.6900	66.0
	200	17.5	0.5833	71.2
	400	12.6	0.4200	79.3
	800	9.3	0.3100	84.7
	1000	5.9	0.1967	90.2
ACA	100	27.1	0.9033	55.4
	200	17.5	0.5833	71.2
	400	13.2	0.4400	78.3
	800	11.3	0.3767	81.4
	1000	9.4	0.3133	84.6

3.3. Potentiodynamic Polarization Method

The linear TAFEL sections of the anodic and cathodic curves were extrapolated to acquire the corrosion current densities from where the corrosion inhibition efficiency, $IE_{PDP}(\%)$ was calculated using the measured corrosion

current density values by adopting the relationship in Equation 1. The Tafel polarization curves for both CHE and ACA are shown in figure 2.

In the presence of *A. galanga* extracts, the corrosion potential, E_{corr} are almost constant; therefore, *A. galanga* extract could be classified as a mixed-type inhibitor. They exhibit characteristics similar to those proposed by Dariva Galio [43] in which inhibitors act as film forming compounds that cause the formation of precipitates on the metal surface thereby blocking both anodic and cathodic sites.

Table 2 shows the electrochemical parameters associated with the polarization behaviour of mild steel in HCl at different concentrations of CHE and ACA. From the tables, the corrosion current (I_{corr}) decreases with increase in the concentration of inhibitor thus leading to increased efficiency. This is as a result of increase in the coverage area of the mild steel by the inhibitor molecules [44].

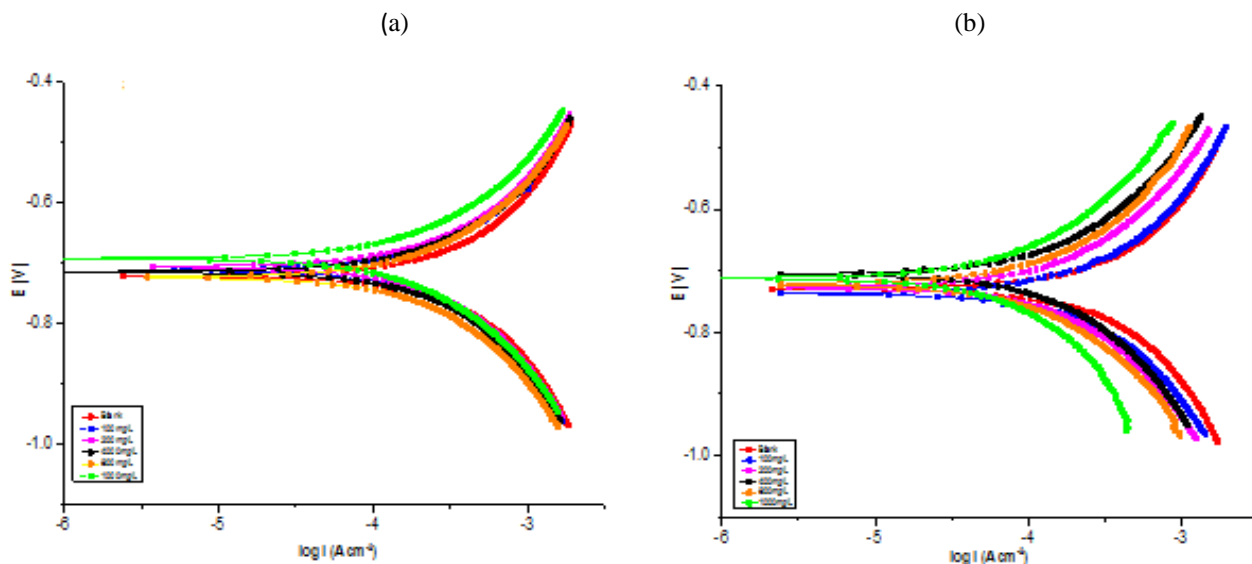


Figure 2: Tafel polarization curves for corrosion of mild steel in absence and presence of different concentrations of (a) CHE and (b) ACA. measurements

Table 2 reveals that CHE and ACA behave as corrosion inhibitors with decrease in corrosion current density on their addition to corrosion solution at all concentrations considered.

Table 2: Tafel Polarization Parameters for Mild Steel in 1M HCl using CHE and ACA

Inh.	Inh. Conc. (ppm)	I_{corr} ($10^{-4} A cm^{-2}$)	b_c (V/dec)	b_a (V/dec)	E_{corr} (V)	R_c (mm/yr)	IE (%)
Blank	0	8.049	0.559	0.512	-0.722	9.355	-
CHE	100	2.982	0.292	0.239	-0.720	3.466	63.0
	200	2.241	0.379	0.257	-0.728	2.605	72.2
	400	2.061	0.242	0.219	-0.693	2.396	74.4
	800	1.393	0.301	0.275	-0.710	1.618	82.7
	1000	0.942	0.297	0.247	-0.722	1.095	88.3
ACA	100	3.585	0.429	0.372	-0.714	5.187	55.5
	200	2.163	0.330	0.290	-0.745	2.514	73.1
	400	2.112	0.310	0.292	-0.706	2.455	73.8
	800	2.054	0.254	0.264	-0.712	2.387	74.5
	1000	1.606	0.306	0.241	-0.721	1.871	80.0

Both the extract and the major active compound of *A. galanga* behave as mixed inhibitors in which both shifts are realized and there is reduction in both the cathodic and anodic reactions. It is also clearly shown that the

inhibition efficiencies of CHE of *A. galanga* extracts and its major constituent, ACA increase with inhibitor concentrations. This also supports the results obtained using weight loss that the extracts of *A. galanga* behave as good inhibitors for the corrosion of mild steel in HCl medium.

3.4. Electrochemical Impedance Spectroscopy

The Nyquist plot representations for various concentrations of CHE and ACA are shown in figure 2. The ZsimpWin electrochemical impedance modelling software was used for data acquisition. Analysis adopting the Randles equivalent circuit model which gave almost semi-circular fit to the experimental studies was used. The R_{ct} values were estimated as the variance between the impedance at lower and higher frequencies.

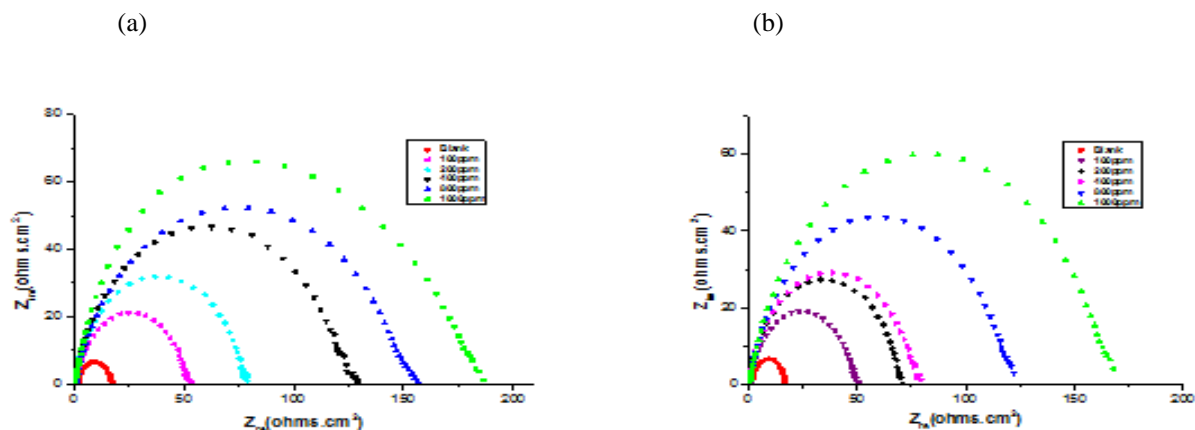


Figure 3: Nyquist plots for corrosion of mild steel in absence and presence of different concentrations of (a) CHE and (b) ACA

The evaluated EIS parameters for the inhibitors are shown in Table 3. A corresponding increase in R_{ct} values with increasing concentrations of CHE and ACA is recorded but there is a contrary trend in the C_{dl} values with increase in R_{ct} values. This is due to decrease in local dielectric constant as a result of increase in the thickness of the electrical double layer. The percentage inhibition efficiencies were calculated from R_{ct} values. The higher the R_{ct} values, the lower is the C_{dl} with attendant increase in surface coverage by the inhibitors on mild steel thereby resulting into an increase in the inhibition efficiency [45, 46].

Table 3: Electrochemical impedance parameters for mild steel in 1 M HCl using CHE and ACA at different concentrations

Inhibitor	Inh. Conc. (ppm)	R_s ($\Omega \text{ cm}^{-2}$)	R_{ct} ($\Omega \text{ cm}^{-2}$)	C_{dl} ($\mu \text{ cm}^{-2}$)	IE (%)
Blank	0	4.25	21.05	8.98	-
CHE	100	5.53	57.65	7.96	63.5
	200	5.98	83.20	7.45	74.7
	400	7.01	91.13	6.91	76.9
	800	7.23	114.40	4.99	81.6
	1000	9.34	173.58	4.55	87.9
ACA	100	4.99	53.29	9.01	60.5
	200	6.54	67.68	7.96	68.9
	400	7.21	88.82	5.90	76.3
	800	8.08	117.60	5.25	82.1
	1000	8.78	135.74	4.73	84.5

Comparing the results of inhibition efficiencies obtained from weight loss, potentiodynamic polarization and electrochemical impedance studies for all the inhibitors at the corresponding concentrations, there are some variations but their results follow similar trend. The difference in the inhibition efficiencies is attributable to the fact that average weight loss values are considered in weight loss measurement while instantaneous corrosion rate values are considered in the electrochemical measurements.

3.5. Quantum chemical methods

The quantum chemical methods are used to support results of the experiments. The density functional theory (DFT) has proved a versatile tool in providing theoretical basis for the interaction process between the molecules of an inhibitor and the metal surface [47, 48]. It has been established that the adsorption of inhibitor molecules on metal surface occurs mainly on the underline condition of donor-acceptor interactions that occur between the nucleophile (π electrons from inhibitor) and the electrophile (vacant d-orbital of the metal) [49]. High values of E_{HOMO} in an inhibitor have been identified as appropriate for good interaction with metal surface. It shows the ability to donate electrons to enhance the adsorption process. On the other hand, the E_{LUMO} gives an indication of the ability of a molecule to accept electrons into its unoccupied orbitals. Lower values of E_{LUMO} portend the molecule's readiness to accept electrons. The energy gap (ΔE) is a relation describing an important stability index of corrosion inhibition. A large energy gap implies high stability of the molecule. Using the various relations established by the works of [50] and [51], the quantum chemical parameters calculated for ACA are presented in Table 4. In the table, the high E_{HOMO} and low E_{LUMO} values with corresponding high energy gap supports the high inhibitive effect of ACA that is obtained experimentally. Analogous reports have been documented as the one reported in this work.

Table 4: Calculated quantum chemical parameters for ACA using DFT at the B3LYP/6-31G(d) level basis set

Quantum Parameters	ACA
E_{HOMO} (eV)	-6.6042
E_{LUMO} (eV)	-0.5127
$\Delta E = E_{LUMO} - E_{HOMO}$ (eV)	6.0915
μ (Debye)	2.2013
$\chi = \frac{IP + EA}{2}$ (eV)	3.5584
$IP = -E_{HOMO}$ (eV)	6.6042
$EA = -E_{LUMO}$ (eV)	0.5127
$\eta = \frac{IP - EA}{2}$ (eV)	3.0458
$s = \frac{1}{\eta} = \frac{2}{IP - EA}$ (eV ⁻¹)	0.3283
$\Delta N = \frac{\chi_{Fe} - \chi_{inh}}{[2(\eta_{Fe} + \eta_{inh})]}$	0.565

The value of fraction of electron transferred, ΔN relates to the ability of the molecule to donate electrons and consequently the efficiency of the inhibitor molecule. The absolute electronegativity (χ) and hardness (η) values of 7.00 eV and 0 eV for Fe respectively were used in calculating the ΔN value [48] The calculated value of 0.57 indicates that ACA is a promising indicator having a high tendency to donate electrons to the surface of the mild steel. In their work, Lukovits.Kálmán Zucchi [52] have shown that, when $\Delta N < 3.6$, there is an increasing tendency of an inhibitor to donate electrons to the metal surface and the inhibition efficiency is enhanced. A similar approach has been adopted to elucidate the feasibility of interaction between ACA and mild steel surface. The low value of ΔN strongly correlates with the experimental inhibition efficiency of ACA.

3.6. Adsorption consideration

The surface coverage data are adopted for fitting experimental data into adsorption isotherms. The types of interaction between the inhibitor molecules and the metal surface are described by the adsorption isotherms [53, 54] The data obtained from the weight loss measurement were used to generate the adsorption isotherms which is represented by Equation 4. The Langmuir adsorption isotherms were the more fitted for the inhibition of extracts molecules on the mild steel surface at the different concentrations of inhibitors used. The Langmuir isotherms assume a direct relationship between inhibition efficiency and the degree of surface coverage (θ) for

different inhibitor concentrations. CHE and ACA obey Langmuir adsorption isotherms by producing straight lines for the plots of C/θ versus concentrations of the inhibitors.

$$\frac{C_{inh}}{\theta} = \frac{1}{K_{ads}} + C_{inh} \quad (5)$$

Where K_{ads} is the binding constant of the adsorption reaction and C_{inh} is the inhibitor concentration in the bulk of the solution.

Plots of C/θ versus Concentrations (Langmuir adsorption plots) produce straight lines with the intercept of each straight line equal to the reciprocal of the binding constant. The adsorption isotherms for the crude extracts of *Alpinia galanga* and ACA are shown in Figure 4.

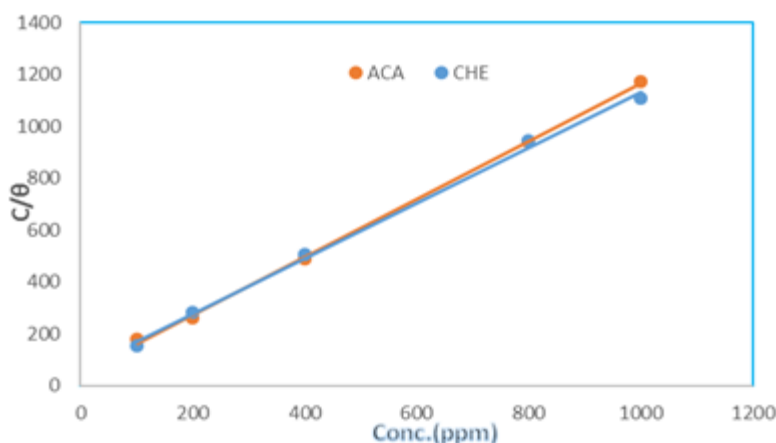


Figure 4: Langmuir Adsorption Isotherm for CHE and ACA at different concentrations

The main process of inhibition is adsorption as revealed by the straight lines obtained in the isotherms. It reveals further that increase in efficiency with increase in concentrations is a clue of increased number of components of the inhibitors adsorbed onto the mild steel surface. The blocking of the active sites on the mild steel surface leads to its protection from corrosion the acid medium.

The K_{ads} values give the strength of adherence between the inhibitors and mild steel. Large K_{ads} values infer more effective adsorption and hence better inhibition efficiency [55]. Table 5 shows the adsorption parameters for the extract and ACA as inhibitors at room temperature.

Table 5: Adsorption parameters for the inhibitors at room temperature ($27 \pm 2^\circ\text{C}$)

Inhibitor	Intercept (ppm)	Slope	R^2	K_{ads} (Lmg^{-1})
CHE	62.6973	1.0706	0.9974	0.0159
ACA	50.1356	1.1180	0.9992	0.0200

As the natural extract contains infinite components at various contents, we may introduce that inhibitory effect is conducted by the intermolecular synergistic effect of several molecules [56-58]. The determination of ΔG_{ads} values has no meaning since the principal component playing the major effect on inhibition process is unknown and content of extract is expressed by ppm and not in mol per liter.

3.7. Surface Characterization (FESEM)

Figures 5 (a) – (d) show for comparison, the images of the mild steel specimens for the polished and surfaces after immersion in inhibited and uninhibited corrosion media. The uninhibited surface appears very rough compared to the inhibited surfaces due to the acid attack. In the presence of CHE and ACA, the rough surface of the metal specimen is smoothed as a result of the protective layer formation on it. The protective layer serves as a barrier in between the mild steel and the acid corrosion media.

The SEM images revealed that the mild steel specimen immersed in inhibited solution is in better condition having a smooth surface while the metal surface immersed in blank acid solutions is rough covered with corrosion products and appeared like full of pits and cavities [53,59].

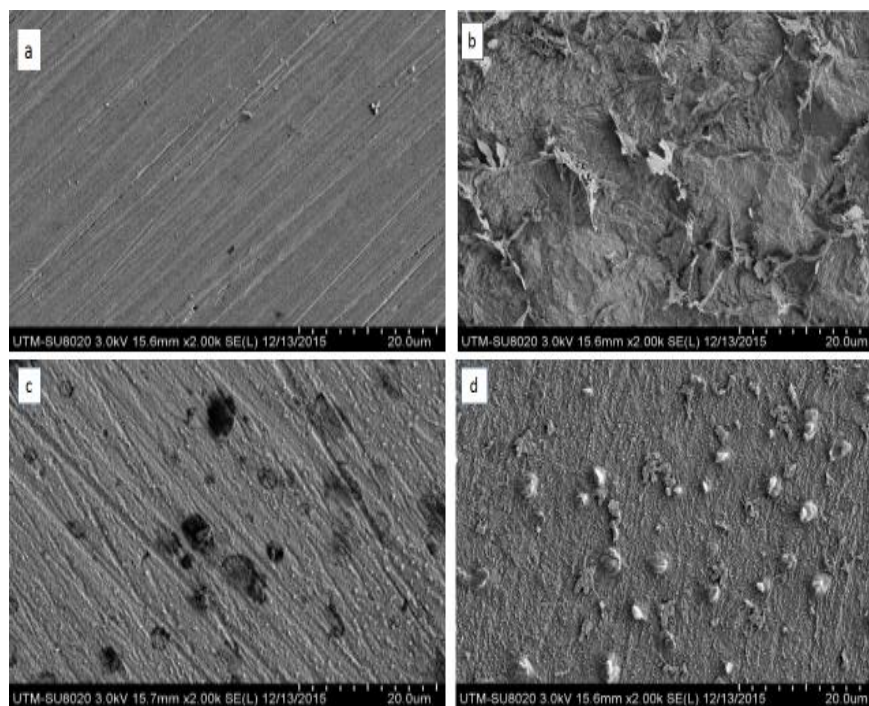


Figure 5: FESEM images of mild steel surfaces (a) polished, (b) after 3 hours of immersion in 1 M HCl, (c) after 3 hours of immersion in CHE and (d) after 3 hours of immersion in ACA

Conclusions

The applicability of *Alpinia galanga* rhizomes as corrosion inhibitor was investigated using its crude hexane extract and its major active constituent namely, 1'-acetochoavicol acetate on mild steel in hydrochloric acid solution. The corrosion inhibition efficiency was established using weight loss, electrochemical and quantum chemical techniques. The potentiodynamic polarization results showed the inhibitors behaving as mixed inhibitors and physisorption was proposed as the adsorption mechanism for the inhibition process. The interaction of the inhibitors on mild steel surface was found to conform to the Langmuir adsorption isotherm. The effectiveness of the inhibitors on mild steel in hydrochloric acid solution was further established using quantum chemical methods and supported by FESEM for surface morphology.

Acknowledgments- The authors acknowledge the Ministry of Higher Education of Malaysia (MOHE), the Research Management Center (RMC) of the Universiti Teknologi Malaysia (UTM) and the grant with VOT No. 4F257.

References

1. Schweitzer P.A., *Fundamentals of corrosion: mechanisms, causes, and preventative methods*: CRC Press, 2009.
2. Abdel-Gaber A.M., Abd-El-Nabey B.A., Sidahmed I.M., El-Zayady A.M., Saadawy M., *Corros. Sci.*, 48 (2006) 2765.
3. Rani B.E.A., Basu B.B.J., *Int. J. Corros.*, 2012 (2012) 1.
4. Oguzie E.E., Li Y., Wang S.G., Wang F., *RSC Advances.*, 1 (2011) 866.
5. Nasibi M., Mohammady M., Ghasemi E., Ashrafi A., Zaarei D., Rashed G., *J. Adhes. Sci. Technol.*, 27 (2013) 1873.
6. Mejeha I.M., Nwandu M.C., Okeoma K.B., Nnanna L.A., Chidiebere M.A., Eze F.C., *et al.*, *J. Mater. Sci.*, 47 (2011) 2559.
7. Khaled K.F., Abdel-Rehim S.S., Sakr G.B., *Arab. J. Chem.*, 5 (2012) 213.
8. Soltani N., Tavakkoli N., Khayat Kashani M., Mosavizadeh A., Oguzie E., Jalali M., *J. Ind. Eng. Chem.*, 20 (2014) 3217.
9. Obi-Egbedi N.O., Obot I.B., Umoren S.A., *Arab. J. Chem.*, 5 (2012) 361.
10. Singh A., Ebenso E.E., Quraishi M.A., *Int. J. Corros.*, 7 (2012) 3409.
11. Li X., Deng S., *Corros. Sci.*, 65 (2012) 299.

12. Deng S., Li X., *Corros. Sci.*, 55 (2012) 407.
13. Ji G., Shukla S.K., Dwivedi P., Sundaram S., Prakash R., *Ind. Eng. Chem. Res.*, 50 (2011) 11954.
14. Hooshmand Zaferani S., Sharifi M., Zaarei D., Shishesaz M.R., *J. Environ. Chem. Eng.*, 1 (2013) 652.
15. Muthumegala T.S., Krishnaveni A., Sangeetha M., Rajendran S., *Zaštita Materijala.*, 1 (2011).
16. Sangeetha M., Rajendran S., Muthumegala T.S., Krishnaveni A., *Zaštita Materijala.*, 1 (2011) 3.
17. Rajalakshmi R., Prithiba A., Leelavathi S., *J. Chemica Acta.*, 1 (2012) 6.
18. Dar M.A., *Ind. Lubr. Tribol.*, 63 (2011) 227.
19. Davis G.D., Fraunhofer J., Krebs L.A., Dacres C.M., Corrosion/2001 Paper 1558. NACE (2001).
20. Muthukrishnan P., Jeyaprabha B., Prakash P., *Arab. J. Chem.*, (2013).
21. Uwah I.E., Okafor P.C., Ebiekpe V.E., *Arab. J. Chem.*, 6 (2013) 285.
22. Singh A., Ahamad I. Quraishi M.A., *Arab. J. Chem.*, (2012).
23. Prabhu D., Rao P., *J. Environ. Chem. Eng.*, 1 (2013) 676.
24. Al-Turkustani A.M., Arab S.T., Al-Qarni L.S.S., *J. Saudi Chem. Soc.*, 15 (2011) 73.
25. Hussin M.H., Jain Kassim M., Razali N.N., Dahon N.H., Nasshorudin D., *Arab. J. Chem.*, (2011).
26. Eduok U.M., Umoren S.A., Udoh A.P., *Arab. J. Chem.*, 5 (2012) 325.
27. Ibrahim T., Alayan H., Mowaqet Y.A., *Prog. Org. Coat.*, 75 (2012) 456.
28. Yaro A.S., Khadom A.A., Wael R.K., *Alexandria Engineering Journal.*, 52 (2013) 129.
29. Deng S., Li X., *Corros. Sci.*, 64 (2012) 253.
30. Akalezi C.O., Enenebaku C.K. Oguzie E.E., *Int. J. Ind. Chem.*, 3 (2012).
31. Garai S., Garai S., Jaisankar P., Singh J.K., Elango A., *Corros. Sci.*, 60 (2012) 193.
32. Lebrini M., Robert F., Lecante A., Roos C., *Corros. Sci.*, 53 (2011) 687.
33. Ostovari A., Hoseinie S.M., Peikari M., Shadizadeh S.R., Hashemi S.J., *Corros. Sci.*, 51 (2009) 1935.
34. Behpour M., Ghoreishi S.M., Khayat Kashani M., Soltani N., *Mater. Chem. Phys.*, 131 (2012) 621-633.
35. Chevalier M., Robert F., Amusant N., Traisnel M., Roos C., Lebrini M., *Electrochim. Acta.*, (2013).
36. Mahae N., Chaiseri S., *Kasetsart J. Nat. Sci.*, 43 (2009) 358.
37. Chan E.W.C., Ng V.P., Tan V.V., Low Y.Y., *Phcog. J.*, 3 (2011) 54-61.
38. Verma R.K., Mishra G., Singh P., Jha K.K., Khosa R.L., *Der Pharmacia Sinica.*, 2 (2011) 142.
39. Fouda A.S., Nazeer A.A., Ibrahim M., Fakhri M., *J. Korean Chem. Soc.*, 57 (2013) 272.
40. Al-Fakhri A., Aziz M. Sirat H., *J. Mater. Environ. Sci.*, 6 (2015) 1480.
41. ASTM. G1-03., Standard practice for preparing, cleaning and evaluating corrosion test specimens (2003).
42. Amira W.E., Rahim A., Osman H., Awang K. Raja P.B., *Int. J. Electrochem. Sci.*, 6 (2011) 2998.
43. Dariva C.G., Galio A.F., "Corrosion Inhibitors—Principles, Mechanisms and Applications," in *Developments in Corrosion Protection*, ed: In Tech, 2014.
44. Krishnaveni K., Ravichandran J., *J. Adhes. Sci. Technol.*, 29 (2015) 1465.
45. Prabakaran M., Kim S., Kalaiselvi K., Hemapriya V., III-Min C., *J. Taiwan Inst. Chem. E.*, 59 (2015) 1.
46. Mayakrishnan G., Pitchai S., Raman K., Vincent A.R., Nagarajan S., *Ionics.*, 17 (2011) 843.
47. Boussalah N., Ghalem S., El Kadiri S., Hammouti B., Touzani R., *Res. Chem. Intermed.*, 38 (2012) 2009.
48. Eddy N.O., Awe F.E., Gimba C.E., Ibisi N.O., Ebenso E.E., *Int. J. Electrochem. Sci.*, 6 (2011) 931.
49. Ebenso E.E., Isabirye D.A., Eddy N.O., *Int. J. Mol. Sci.*, 11 (2010) 2473.
50. Pearson R.G., *Inorg. Chem.*, 27 (1988) 734.
51. Parr R.G. Pearson R.G., *J. Am. Chem. Soc.*, 105 (1983) 7512.
52. Lukovits I., Kálmán E., Zucchi F., *Corrosion.*, 57 (2001) 3.
53. Leelavathi S., Rajalakshmi R., *J. Mater. Environ. Sci.*, 4 (2013) 625.
54. Hosseini M., Mertens S.F., Arshadi M.R., *Corros. Sci.*, 45 (2003) 1473.
55. Li X., Deng S., Fu H., Mu G., *Corros. Sci.*, 51 (2009) 620.
56. Dahmani M., Et-Touhami A., Al-Deyab S.S., Hammouti B., Bouyanzer A., *Int. J. Electrochem. Sci.*, 5 (2010) 1060- 1069.
57. Bouknana D., Hammouti B., Messali M., Aouniti A., Sbaa M., *Port. Electrochim. Acta*, 32 (2014) 1-19.
58. Ali A.I., Megahed H.E., El-Etre M.A., Ismail M.N., *J. Mater. Environ. Sci.* 5 (2014) 923-930
59. Bouoidina A., El-Hajjaji F., Chaouch M., Abdellaoui A., Elmsellem H., Rais Z., Filali Baba M., Lahkimi A., Hammouti B. and Taleb M., *Der Pharma Chemica*, 8(13) (2016)149-157

(2017) ; <http://www.jmaterenvirosci.com>